Original Article

The effects of cutouts on output, mean energy and percentage depth dose of 12 and 14 MeV electrons

Navid Khaledy[1,2], Azim Arbabi[2], Dariush Sardari[3]

[1]Young Researchers Club, Science and Research Branch, Islamic Azad University, [2]Department of Medical Physics, Imam Hosein Hospital, Shahid Beheshti Medical University, Tehran, Iran, [3]Department of Medical Radiation, Islamic Azad University, Science and Research Branch, Tehran, Iran

Received on: 27.02.11 **Review completed on: 11.04.11** **Accepted on: 21.07.11**

ABSTRACT

Electron field-shaping cerrobend cutouts on the linear accelerator applicator have some effects on the output and percentage depth dose. These effects which arise from the lateral scatter nonequilibrium are particularly evident in higher energies and in cutouts with smaller radius. Dose measurements for circular, square, and triangular cutouts as well as open field was performed in a 10 × 10 cm applicator, using plane parallel type ion chamber with a 100 cm source surface distance. The Percentage Depth Doses curves were drawn and the outputs were measured for each of these cutouts. The output factors, normalized to open 10 × 10 cm field, varied between 0.891 and 0.996 depending on the energy, cutout shape, and cavity area. With the use of cutouts, R_{100} shifted toward the surface. The shifts ranged from 9 to 0 mm and from 13 to 0 mm for 12 and 14 MeV, respectively, depending on the shape and cavity area. For R_{90}, R_{80}, and R_{50} the ranges for observed shifts narrowed down and practically no shifts were observed for R_{20}. We present these changes in the form of predictive formulas, which would be useful in clinical applications.

Key words: Cutout, electron beam, formulization, output factor, profile, percentage depth dose

Introduction

In treatment of cancers using electron beams, depending on the type and the shape of tumor, cast cerrobend alloy cutouts are used. Cerrobend is a fusible alloy usually containing of Tin, Lead, Bismuth, and Cadmium. We used the cadmium-free type.

The cutouts change the percentage depth dose (PDD) and the output,[1-3] in a way that the slope of descending part of PDD curve increases. Therefore, the values for R_{100}, R_{90}, R_{80}, and R_{50} in order show the highest decrease. Also $E_{0(mean)}$ and OPF decrease while the cutout cavity area decreases.[4,5]

These changes in higher energy and smaller diameter cutouts are more profound, which is arising from the lack of lateral scatter equilibrium. R_{eq} (minimum radius for the establishment of lateral scatter equilibrium) is calculated using the following equations:[6]

$$R_{eq} \approx 0.88 \times \sqrt{E_{p0}} \quad \text{.....(1)}$$

In this formula, E_{p0} is the most probable energy at the phantom surface for the reference field size:[7,8]

$$E_{p0} = 0.22 + 1.98R_p + 0.0025R_p^2 \quad \text{.....(2)}$$

In radius smaller than R_{eq} values of R_{100}, R_{90}, R_{80}, R_{50}, $E_{0(mean)}$, and OPF are expected to change.[2]

The main aim of this study was to fit the values of R_{100}, R_{90}, R_{80}, R_{50}, $E_{0(mean)}$, and OPF changes on a curve and formulizing these changes as a function of cutouts cavity area. There in this way there will be no need to carry on dosimetry for each patient individually.[2,9]

Address for correspondence:
Mr. Navid Khaledy,
Department of Radiotherapy, Imam Hossain Hospital, Madani St., Tehran, Iran.
E-mail: navidkhaledy@gmail.com

Access this article online

Quick Response Code:

Website: www.jmp.org.in

DOI: 10.4103/0971-6203.89970

Materials and Methods

Dosimetry system

We used PTW (PTW Freiburg, Germany) hardware and software. The water phantom used had a 50 × 50 × 50 cm size and the model was MP3. A plane parallel-type chamber was used for absolute and relative dosimetry, and a thimble-type chamber was used as a reference chamber and was placed outside of the phantom near the radiation field corner. The plane parallel chamber model was PTW 34045 and its sensitive volume was 0.02 cm^3. The cylindrical chamber model was PTW 31010. Controller software and collected data compiler was the MEPHYSTO® mc2. The IAEA TRS398 dosimetry protocol was used in this study.[10]

Dosimetry

Dosimetry was performed in 100 cm source surface distance (SSD) and using a 10 × 10 cm applicator. Dosimetry setup used for our work is shown in Figure 1. The PDD curve and output for the square, circle, and triangle cutouts and the 10 × 10 cm reference field was measured. The opening of X-ray jaws was 19 × 19 cm. Linear accelerator used was a Siemens Primus model and the results were for the 12 and 14 MeV energies. The circle cutout diameters were 3, 4, 5, 6, and 8 cm. Squares had side lengths of 2.66, 3.54, 4.43, 5.32, and 7.1 cm. Also the equilateral triangles had 4.05, 5.4, 6.75, 8.1, and 10.58 cm side lengths. The cavity areas from the smallest cutout to the largest one for each shape were 7.06, 12.56, 19.62, 28.26, and 50.24 cm^2, respectively.

To obtain PDD both chambers were on. The obtained curves were the percentage depth ionization (PDI) and then converted to the PDD by MEPHYSTO® mc2 software. After the percentage depth dose curves were drawn, the information were extracted as R_{100}, R_{90}, R_{80}, R_{50}, R_{20}, R_p, and $E_{0(mean)}$.

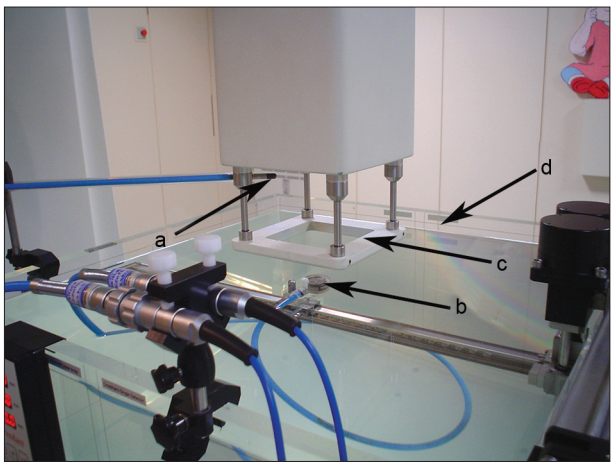

Figure 1: Dosimetry setup in Mahak Hospital Department of Radiation Therapy used for our work. (a) The thimble chamber was used as the reference chamber, (b) the plane parallel chamber moves along the central axis for PDD measurements, or would be fixed at dmax for output measurements, (c) bottom of the applicator, the place of cutout insertion, and (d) The water phantom

The mean energy of the electron field in the phantom surface was calculated by Eq. (3).[7,8]

$$E_{0(mean)} = C_4 \times R_{50}, C_4 = 2.33 \text{ MeV cm}^{-1} \quad \text{.....(3)}$$

For measuring the output, the plane parallel chamber was placed at the depth of maximum dose. The maximum depth dose was calculated for each cutout using the PDD curve, because the cutouts' d_{max} are different to a 10 × 10 cm field.

We measured the output after turning off the thimble chamber. The measurement was done four times for each field and the average was compared with the reference field (10 × 10 cm) output.

Results

Percentage depth dose curves

Percentage depth dose curve on the central axis for 12 MeV energy

We calculated R_p using PDD curve, which was equal to 5.7 cm and using the Eq. (2) the E_{p0} was 11.53 MeV. Also the minimum radius required for lateral scatter equilibrium in 12 MeV electron energy by using Eq. (1) was about 3 cm. Meaning the minimum circular field diameter necessary for 12 MeV electron lateral scatter equilibrium establishment is about 6 cm, which means that changes in PDD for circular field with diameter of less than 6 cm are expected.[2]

As is clear from Table 1, shields cause more change in higher depth doses, especially R_{100}, R_{90}, and R_{80}, and it has a little effect (up to 1 mm) on the R_{20}, which is negligible. Triangular shields changed R_{100}, R_{90}, R_{80}, and R_{50} more than the circular and square shields. The reduction in R_{100} in the triangle shield was from 27 to 18 mm, but for the circular and square shield it was from 27 to 19 mm. For circular and square fields larger than 28.26 cm^2, due to the establishment of electron lateral scattering equilibrium effect there is no difference between the values of R_{100}, R_{90}, R_{80}, and R_{50} compared to reference field. Also, the mean energy of the electron field in smaller fields is lower.

By fitting these values on the curve, we devised Eq. (4) (8) formulas to calculate the parameter change based on cutouts area.

Dynamic fit curve was found to be the best method for matching above-mentioned values on a proper curve and attaining its computed formula. With formulization of these changes for R_{100}, Eq. (4) was obtained:

$$R_{100} = 26.7 + \frac{47.2}{s} - \frac{1918}{s^2} + \frac{8340}{s^3} \quad \text{.....(4)}$$

This formula is a Polynomial type, where *S* is the area of the shield cavity.

Other methods, such as A/P[11] in which A is the area of the cavity and *P* is the periphery of the cutout hole, were not utilized due to the lack of favorable results in formulization.

For R_{90}, R_{80}, and R_{50} these equations were calculated:

$$R_{90} = 36.4 + \frac{71.8}{s} - \frac{1790}{s^2} + \frac{6313}{s^3} \quad \text{.....(5)}$$

$$R_{80} = 39.6 + \frac{47.4}{s} - \frac{1104}{s^2} + \frac{3216}{s^3} \quad \text{.....(6)}$$

Table 1: Values obtained from percentage depth dose curve for each of the three field shapes (12 MeV)

	Area (cm^2)	*R_{100} (mm)*	*R_{90} (mm)*	*R_{80} (mm)*	*R_{50} (mm)*	*R_{20} (mm)*	*$E_{0(mean)}$ (MeV)*
Circle	7.06	19	29	34	44	52	10.10
	12.56	23	34	38	46	53	10.67
	19.62	25	36	40	47	53	10.92
	28.26	27	37	40	47	53	10.91
	50.24	27	37	40	47	53	10.92
Square	7.06	19	29	33	43	52	10.05
	12.56	23	34	38	46	53	10.56
	19.62	25	36	40	47	53	10.94
	28.26	27	37	40	47	53	10.92
	50.24	27	37	40	47	53	10.93
Triangle	7.06	18	28	33	43	52	10.37
	12.56	22	34	38	46	53	10.55
	19.62	25	36	39	47	53	10.87
	28.26	26	37	40	47	53	10.89
	50.24	27	37	40	47	53	10.91
Mean (including the standard deviations)	7.06	19 ± 1	29 ± 1	33 ± 1	43 ± 1	52 ± 0	10.17 ± 0.13
	12.56	23 ± 1	34 ± 0	38 ± 0	46 ± 0	53 ± 0	10.59 ± 0.07
	19.62	25 ± 0	36 ± 0	40 ± 1	47 ± 0	53 ± 0	10.91 ± 0.04
	28.26	23 ± 1	37 ± 0	40 ± 0	47 ± 0	53 ± 0	10.91 ± 0.02
	50.24	27 ± 0	37 ± 0	40 ± 0	47 ± 0	53 ± 0	10.92 ± 0.01
10 x 10	100	27	37	40	47	53	10.96

Table 2: Values obtained from percentage depth dose curve for each of the three field shapes (14 MeV)

	Area (cm^2)	*R_{100} (mm)*	*R_{90} (mm)*	*R_{80} (mm)*	*R_{50} (mm)*	*R_{20} (mm)*	*$E_{0(mean)}$ (MeV)*
Circle	7.06	20	31	36	47	57	10.90
	12.56	24	37	41	50	58	11.60
	19.62	27	39	43	51	59	12.02
	28.26	27	40	44	52	59	12.09
	50.24	29	40	44	52	59	12.13
Square	7.06	19	31	35	46	57	10.80
	12.56	24	36	41	51	58	11.34
	19.62	26	39	43	51	59	11.98
	28.26	28	40	44	52	59	12.03
	50.24	30	40	44	52	59	12.12
Triangle	7.06	17	29	35	46	57	10.71
	12.56	23	35	40	50	58	11.06
	19.62	25	38	43	51	59	11.95
	28.26	28	39	43	51	59	11.97
	50.24	29	40	44	52	59	12.09
Mean (including the standard deviations)	7.06	19 ± 2	30 ± 1	35 ± 1	46 ± 1	57 ± 0	10.80 ± 0.10
	12.56	24 ± 1	36 ± 1	41 ± 1	50 ± 1	58 ± 0	11.33 ± 0.17
	19.62	26 ± 1	39 ± 1	43 ± 0	51 ± 0	59 ± 0	11.98 ± 0.04
	28.26	28 ± 1	40 ± 1	44 ± 1	52 ± 1	59 ± 0	12.03 ± 0.06
	50.24	29 ± 1	40 ± 0	44 ± 0	52 ± 0	59 ± 0	12.11 ± 0.02
10 × 10	100	30	40	44	52	59	12.19

$$R_{50} = 46.7 + \frac{31}{s} - \frac{641}{s^2} + \frac{1784}{s^3} \quad \text{.....(7)}$$

$$E_{0(mean)} = 10.95 \times e^{-e^{-\left(\frac{s+8.4}{5.96}\right)}} \quad \text{.....(8)}$$

In the formula for $E_{0(mean)}$, the fitted curve was a Sigmoidal (Gompertz) type.

Percentage depth dose curve on the central axis for 14 MeV energy

Here the R_p was equal to 6.2 cm and the E_{p0} was 12.66 MeV. As a result $R_{eq} = 3.2$ cm.

PDD data for 14 MeV is demonstrated in Table 2.

In this energy the highest change was observed in R_{100}. Here again the decrease on R_{100}, R_{90}, R_{80}, and R_{50} by the triangular shields is rather than circular and square shields. The R_{100} for the circular shape decreased from 30 to 20 mm in comparison with the reference field. For the square cutout it changed from 30 to 19 mm and for triangle cutout it changed from 30 to 17 mm. The R_{20} for the 7.06 cm^2 area for all fields reduced from 59 to 57 mm.

In the largest area (50.24 cm^2) for 14 MeV in the circular and triangle fields the change of R_{100} was 1 mm and for the square cutout it remained unchanged.

For 14 MeV similar to 12 MeV the mean energy for smaller fields was lower than the larger fields. The maximum reduction in mean energy was for the triangle shape, decreasing from 12.19 to 10.71 MeV.

Figures 2–4 are obtained by fitting the Mean values of Tables 1 and 2 on the curves. In these figures, the error bars represent plus and minus standard deviations for each point. Some points have same value in several measurements, for these points the standard deviations are zero and no error bar exists.

$$R_{100} = 31 - \frac{103.8}{s} + \frac{155.7}{s^2} - \frac{282}{s^3} \quad \text{.....(9)}$$

$$R_{90} = 39.6 + \frac{57.8}{s} - \frac{1841}{s^2} + \frac{6850}{s^3} \quad \text{.....(10)}$$

$$R_{80} = 43.7 + \frac{47.8}{s} - \frac{1475}{s^2} + \frac{5102}{s^3} \quad \text{.....(11)}$$

$$R_{50} = 52.2 - \frac{21.9}{s} + \frac{102.7}{s^2} - \frac{1710}{s^3} \quad \text{.....(12)}$$

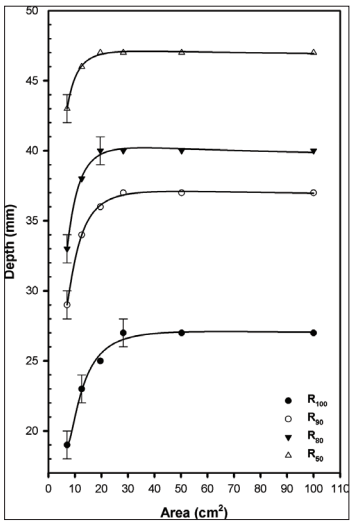

Figure 2: Central axis depth dose parameters changes as a function of the area for 12 MeV

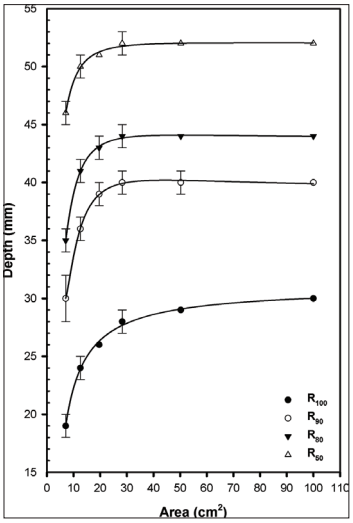

Figure 3: Central axis depth dose parameters changes as a function of the area for 14 MeV

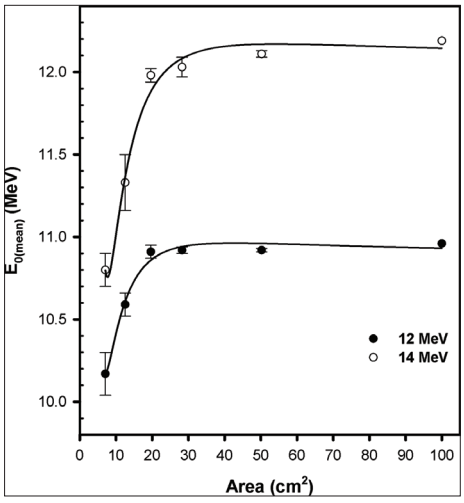

Figure 4: $E_{0(mean)}$ change as a function of the area

$$E_0 = 12.2 \times e^{-e^{-(\frac{s+10.7}{8.5})}} \quad \text{.....(13)}$$

Output factor

Output factor in 12 MeV energy

Dose rates in Gy/min were measured at the depth of maximum for all fields and then calculated as a ratio of the reference dose rate value to obtain the OPF for each shield. The dose rates were measured 4 times for each field.

Averaging the output values in Table 3 can provide a more general formula for all forms:

$$OPF = 1 - 0.186 \times e^{-0.087 \times s} \quad \text{.....(14)}$$

As the cutout area becomes smaller the dose rate and consequently the OPF for the circle, square, and triangle are reduced from 0.993 to 0.907, from 0.995 to 0.895, and from 0.992 to 0.891, respectively. The lowest output was observed for the triangle. Eq. (14) is a more general formula and can be used for all shapes.

Output factor in 14 MeV energy

Here again, the average of OPF values for Table 4 can be used to make a more general formula for all forms in 14 MeV:

$$OPF = 1 - 0.142 \times e^{-0.077 \times s} \quad \text{.....(15)}$$

Eqs (14) and (15) are the formulas for the Figure 5 curves, which were obtained from Tables 3 and 4 data. The curves in Figure 5 are very close together; hence the error bars have had overlap, so the error bars are omitted. However, the standard deviations are available in Tables 3 and 4.

Discussion

The chart of changes for R_{100}, R_{90}, R_{80}, and R_{50} shows that while increasing the shield cavity area, after a certain area the values of these parameters reach a saturation status. This means that there is a threshold for the field size influence on R_{100}, R_{90}, R_{80} and $R_{50.}$ This threshold is close to the R_{eq}.[2,6]

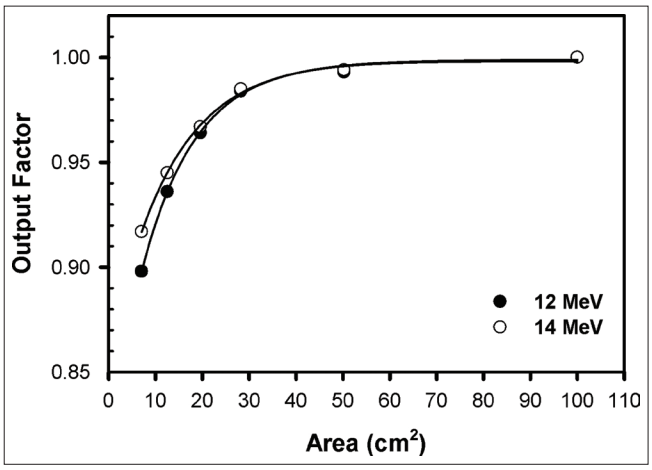

Figure 5: Output factor changes for cutouts with different areas

Table 3: d_{max} and output factor for each of the three shapes and reference field for 12 MeV

Area (cm^2)	*d_{max} (mm) circle*	*d_{max} (mm) square*	*d_{max} (mm) triangle*	*OPF circle*	*OPF square*	*OPF triangle*	*Mean OPF (including the standard deviations)*
7.06	19	19	18	0.907	0.895	0.891	0.898 ± 0.008
12.56	23	23	22	0.933	0.949	0.925	0.936 ± 0.012
19.62	25	25	25	0.961	0.977	0.953	0.964 ± 0.012
28.26	27	26	26	0.984	0.988	0.981	0.984 ± 0.003
50.24	27	27	27	0.993	0.995	0.992	0.993 ± 0.001
100		27			1.000		1.000

OPF: Output factor

Table 4: d_{max} and output factor for each of the three shapes and reference field for 14 MeV

Area (cm^2)	*d_{max} (mm) circle*	*d_{max} (mm) square*	*d_{max} (mm) triangle*	*OPF circle*	*OPF square*	*OPF triangle*	*Mean OPF (including the standard deviations)*
7.06	20	19	17	0.922	0.915	0.915	0.917 ± 0.004
12.56	24	24	23	0.945	0.955	0.934	0.945 ± 0.011
19.62	27	26	25	0.969	0.971	0.961	0.967 ± 0.005
28.26	27	28	28	0.988	0.985	0.981	0.985 ± 0.004
50.24	29	30	29	0.996	0.994	0.991	0.994 ± 0.003
100		30			1.000		1.000

OPF: Output factor

Su *et al*. measured the cutout OPF for 6 MeV electron beam by radiographic film and 2D small volume ion chamber array. The aim of their study was not about the cutout effects on the output, but in their research this effect can also be observed.[1]

Xu *et al*. have demonstrated that for 6 MeV beam and circular cutout, reducing the diameter reduces the amount of R_{100}, R_{50}, and OPF.[2] Besides, Sharma *et al*. observed similar changes in R_{100}, R_{90}, and R_{50} for quadrangular cutouts and 6 MeV energy, due to the changes of R_{100}, they propose using of bolus to decrease the skin dose arisen by the reduction of d_{max}.[12] Zhang *et al*. found that the OPF in 6, 12, 20, 30, and 40 MeV for circular cutouts is reduced when the field radius is smaller than the minimum needed radius for the establishment of lateral scatter equilibrium.[13]

Sharma *et al*. instead of R_{eq} did their measurements for several cutouts with a radius less or more than R_p. For 6 MeV electron beam the difference between the amount of R_p and R_{eq} is about 9 mm, however, in their study the exact threshold of change had not been investigated.[12] Other researchers got the same result for other energies in different methods.[3,4,9,11]

Our findings are in line with the mentioned studies except that these studies have been limited to a particular shape (circular or square) and mostly for one energy level, and none of them have formulized the changes caused by using different cutouts.

In 12 MeV and 50.24 cm^2 area for circular, square, and triangle shapes the values of R_{100}, R_{90}, R_{80}, R_{50}, and R_{20} are equal to the values of the 10 × 10 cm field. The most changes in PDD parameters was observed for the triangle shape, so that R_{100} and R_{90} for 7.06 cm^2 area were changed 1 mm more in comparison with circle and square shapes.

In 14 MeV, the minimum radius for establishment of lateral scatter equilibrium was increased. So, in the 50.24 cm^2 area, which had the largest radius, the R_{100} for both the circular and the triangle shapes was different to the 10 × 10 cm field. For the triangle the R_{90}, R_{80}, and R_{50} values were different from the 10 × 10 cm field. Here again the most changes in the values of R_{100}, R_{90}, R_{80}, R_{50}, and R_{20} were observed with the triangle.

$E_{0(mean)}$ will decrease, if the cutout size is reducing. Whereas $E_{0(mean)}$ is related to the R_{50}, the reduction of R_{50} would cause reduction in $E_{0(mean)}$ as well.

The minimum value of $E_{0(mean)}$ in 12 and 14 MeV was achieved by using 7.06 cm^2 square and 7.06 cm^2 triangle cutouts, respectively, which was equal to 10.05 MeV for 12 MeV and 10.71 MeV for 14 MeV.

The reason why the output and percentage depth dose for triangle are different to circular and square shapes is arising from the nature of the triangle which has smaller width of field in the corners in comparison to square and circle fields, which prevents the establishment of lateral scatter equilibrium more than circular and square shapes.

Conclusions

It is clear that if we use smaller cutouts, in higher depth doses (R_{100}, R_{90}, R_{80}, and R_{50}), more reduction of depth would be seen.[2,12] However, this reduction is much more tangible in the depth of R_{100} and R_{90}.

Considering the d_{max} changes due to the small cutouts, it is obvious that the chamber should be placed at the correct d_{max} in output measurements.[12]

The output of the machine which is one of the most important factors in treatment, decreases with reducing the diameter of cutout.[1,2,9,12] This reduction is more pronounced for triangles rather than circle or square. Also, the changes in PDD and outputs in clinical cases must be considered. For example, to compensate the changes of d_{max}, the bolus might be used[12] and output changes should be considered in the treatment calculation.

The formulas presented in this study, are clinically useful to calculate the changes of PDD and OPF for each regular and semi-regular geometry cutouts on the central axis.

Knowledge of these variations might be effective in having an accurate dosimetry and treatment.

Acknowledgment

We thank Dr. Kourosh Sheibani the chief researcher at Clinical Research and Development Centre, Imam Hossein Medical Centre, for his valuable assistance in preparing and revising the manuscript. We would like to appreciate Mr. Mehdi Goodarzi for editing some parts of the manuscript.

References

1. Su M, Li T, Tong S, Grant D, Farhangi E, Tapen E, *et al*. Small electron field cut-out output factors measured using a 2D ion chamber array compared to radiographic film. Vol. 32. 47th AAPM Annual Meeting; 2005 Jul 24-28; Washington, USA. Med Phys 2005. p. 2007.
2. Xu MM, Sethi A, Glasgow GP. Dosimetry of small circular fields for 6-MeV electron beams. Med Dosim 2009;34:51-6.
3. Bruinvis IA, Van Amstel A, Elevelt AJ, Van der Laarse R. Calculation of electron beam dose distributions for arbitrarily shaped fields. Phys Med Biol 1983;28:667-83.
4. Niroomand-Rad A, Gillin MT, Kline RW, Grimm DF. Film dosimetry of small electron beams for routine radiotherapy planning. Med Phys 1986;13:416-21.
5. Khan FM. The physics of radiation therapy. 3rd ed. Philadelphia: Lippincott Williams and Wilkins; 2003. p. 292-4.
6. Khan FM, Higgins PD, Gerbi BJ, Deibel FC, Sethi A, Mihailidis DN. Calculation of depth dose and dose per monitor unit for irregularly shaped electron fields. Phys Med Biol 1998;43:2741-54.

7. Khan FM, Doppke KP, Hogstrom KR, Kutcher GJ, Nath R, Prasad SC, *et al*. Clinical electron-beam dosimetry: Report of AAPM Radiation Therapy Committee Task Group No. 25. Med Phys 1991;18:73-109.
8. Khan FM. The physics of radiation therapy. 3rd ed. Philadelphia: Lippincott Williams and Wilkins; 2003. p. 267-8.
9. Aggarwal LM, Oommen S, Parthiban V, Passi K, Vashistha R, Bhupinder S. Variation in electron output and percentage depth dose in presence of lead cut-outs in Mevatron-74. J Med Phys 1999;24:44-6.
10. Andreo P, Burns DT, Hohlfeld K, Huq MS, Kanai T, Laitano F, *et al*. Absorbed dose determination in external beam radiotherapy: An international code of practice for dosimetry based on standards of absorbed dose to water. IAEA Technical Report Series no 398. Vienna: International Atomic Energy Agency; 2000.
11. Niroomand-Rad A. Film dosimetry of small elongated electron beams for treatment planning. Med Phys 1989;16:655-62.
12. Sharma SC, Johnson MW, Gossman MS. Practical considerations for electron beam small field size dosimetry. Med Dosim 2005;30:104-6.
13. Zhang GG, Rogers DW, Cygler JE, Mackie TR. Monte Carlo investigation of electron beam output factors versus size of square cut-out. Med Phys 1999;26:743-50.

How to cite this article: Khaledy N, Arbabi A, Sardari D. The effects of cutouts on output, mean energy and percentage depth dose of 12 and 14 MeV electrons. J Med Phys 2011;36:213-9.
Source of Support: Nil, **Conflict of Interest:** None declared.